Anal. Chem. **2002,** *74,* 1497−1502

Detection of Ultratrace Phosphorus and Sulfur by Quadrupole ICPMS with Dynamic Reaction Cell

Dmitry R. Bandura,* Vladimir I. Baranov, and Scott D. Tanner

PerkinElmer-SCIEX, 71 Four Valley Drive, Concord, Ontario L4K 4V8, Canada

A method of detection of ultratrace phosphorus and sulfur that uses reaction with O_2 in a dynamic reaction cell (DRC) to oxidize S^+ and P^+ to allow their detection as SO^+ and PO^+ is described. The method reduces the effect of polyatomic isobaric interferences at $m/z = 31$ and 32 by detecting P^+ and S^+ as the product oxide ions that are less interfered. Use of an axial field in the DRC improves transmission of the product oxide ions 4−6 times. With no axial field, detection limits (3σ, 5-s integration) of 0.20 and 0.52 ng/mL, with background equivalent concentrations of 0.53 and 4.8 ng/mL, respectively, are achieved. At an optimum axial field potential (200 V), the detection limits are 0.06 ng/mL for P and 0.2 ng/mL for S, respectively. The method is used for determining the degree of phosphorylation of β-casein, and regular and dephosphorylated α-caseins at 10−1000 fmol/μL concentration, with 5−10% v/v organic sample matrix (acetonitrile, formic acid, ammonium bicarbonate). The measured degree of phosphorylation for β-casein (4.9 phosphorus atoms/molecule) and regular α-casein (8.8 phoshorus atoms/molecule) are in good agreement with the structural data for the proteins. The P/S ratio for regular α-casein (1.58) is in good agreement with the ratio of the number of phosphorylation sites to the number of sulfur-containing amino acid residues cysteine and methionine. The P/S ratio for commercially available dephosphorylated α-casein is measured at 0.41 (∼26% residual phosphate).

Quantitative determination of phosphorus in biological samples can yield important information about the state of phosphorylation of proteins. The preferred method of phosphorus detection is radioisotope (γ-^{32}P) labeling with scintillation counting.[1] Multiphoton (MPD) detection[2] is a new technology that potentially can improve sensitivity of ^{32}P and ^{35}S detection by several orders of magnitude. These methods have an obvious drawback—the necessity of radioisotope handling and disposal.

Of all other methods used for detection of P and S, sector field ICPMS is the most sensitive. Application of inductively coupled plasma mass spectrometry to $^{31}P^+$ detection in an eluent of micro-LC was described recently.[3,4] Interferences caused by polyatomic ions that originate from N, O, H, and C derived from the sample matrix were reduced by employing a membrane desolvation system (for use with quadrupole ICPMS) or by resolving the interferences spectrally with medium (4000)-resolution sector field ICPMS.[4] The latter achieved a limit of detection of 0.1 pmol at 4 μL/min infusion of aqueous solution, and subnanogram per milliliter detection of $^{31}P^+$ in 3% acetonitrile. Despite the fact that a hexapole collision cell pressurized with H_2 was employed for $m/z = 31$ background reduction in quadrupole ICPMS, the desolvation system was necessary to enable phosphorus detection at submicrogram per milliliter concentrations, due to the high abundance of $^{15}N^{16}O^+$ and $^{14}N^{16}O^1H^+$. It was noted that some compounds were suppressed due to possible loss in the membrane desolvation system. As a result, high-resolution ICPMS was used instead, with low solvent load on the plasma by use of micro-LC at 4 μL/min ensuring good detection limits for P. Detection of the sulfur isotopes $^{32}S^+$ and $^{34}S^+$ was described in ref 5. Use of a He−H_2−Xe mixture in a hexapole collision cell reduced the background at $m/z = 32$ to ∼1 μg/mL and allowed detection limits of 20−50 ng/mL for sulfur.

High-resolution sector field ICPMS employed for measurements of sulfur isotopes provided excellent detection limits of <0.01 ng/mL[6] but required the use of membrane desolvation. It was shown that, without solvent removal, the relatively poor abundance sensitivity of magnetic sector field instruments limits the background equivalent concentration to ∼10 ng/mL even at a resolution of 4500.[7]

In a recent publication, simultaneous measurement of phosphorus and sulfur in proteins by ICPMS was reported.[8] Sector field ICPMS was used at a medium resolution of 4000, with low solvent load on the plasma by use of micro-LC at 4 μL/min ensuring good detection limits for P^+ and S^+.

We have developed a method with which ^{31}P and ^{32}S can be detected by quadrupole ICPMS at subnanogram per milliliter levels, to be used for determination of the degree of phosphorylation of proteins in biological samples. The method is based on chemical resolution of $^{31}P^+$ and $^{32}S^+$ from polyatomic ions by oxidation to $^{31}P^{16}O^+$ and $^{32}S^{16}O^+$ in reaction with oxygen gas supplied to the dynamic reaction cell (DRC). The oxide ions are

(1) Wilson, K.; Walker, J. *Principles and Techniques of Practical Biochemistry*; Cambridge University Press: New York, 2000; pp 319−322.
(2) . Godovac-Zimmerman, J.; Brown, L. R. *Mass Spectrom. Rev.* **2001**, *20*, 1−57.
(3) Siethoff, C.; Feldmann, I.; Jakubowski, N.; Linscheid, M. J. *Mass Spectrom.* **1999**, *34*, 421−426.
(4) Wind, M.; Edler, M.; Jakubowski, N.; Linscheid, M.; Wesch, H.; Lehmann, W. D. *Anal. Chem.* **2001**, *73*, 29−35.
(5) Mason, P. R. D.; Kaspers, K.; van Bergen, M. J. *J. Anal. At. Spectrom.* **1999**, *14*, 1067−1074.
(6) Prohaska, T.; Latkoczy, C.; Stingeder, G. *J. Anal. At. Spectrom.* **1999**, *14*, 1501−1504.
(7) Wildner, H. *J. Anal. At. Spectrom.* **1998**, *13*, 573−578.
(8) Wind, M.; Wesch, H.; Lehmann, W. D. *Anal. Chem.* **2001**, *73*, 3006−3010.

10.1021/ac011031v CCC: $22.00
Published on Web 02/23/2002

Table 1. Thermochemical Properties of Analyte and Interfering Ions

ion	ionization potential, eV	affinity, kcal/mol	
		O-atom	H-atom
P^+	10.486	190.6	78.1
S^+	10.36	125.4	84.7
NO^+	9.26	61.93	31.1
NOH^+	10.1	99.9	83.8
O_2^+	12.07	17.1	66.4

Table 2. Thermochemical Properties of Possible Reaction Gases

neutral	ionization potential, eV	bond strength, kcal/mol	
		O-bond	H-bond
H_2	15.426		104.2
NH_3	10.16		108.2
CH_4	12.51		104.7
C_2H_4	10.507		48.5
C_2H_6	11.52		80.33
N_2O	12.886	40	
O_2	12.07	119.2	
Xe	12.13		

then used as analyte ions. Both S and P are measured in the same measurement under the same instrument operating conditions. This opens the possibility of using S as an internal standard for P in determination of the state of phosphorylation of proteins. For homologous proteins containing cysteine, methionine, or both, sulfur as an internal standard can compensate for variability in the protein concentration of different samples.

Chemical Resolution of Polyatomic Interferences on $^{31}P^+$ and $^{32}S^+$. The main polyatomic interferences at $m/z = 31$ are $^{15}N^{16}O^+$, $^{14}N^{16}O^1H^+$, and $^{12}C^1H_3{}^{16}O^+$, with approximate partition of 15:8:1 and combined $^{31}P^+$ background equivalent concentration of ~500 ng/mL for a 3% acetonitrile sample matrix.[4] Although the exact distribution and equivalent concentration of the interferences are instrument-dependent, the above-mentioned ions are most certainly dominant and thus their suppression must be considered. For $^{32}S^+$, the dominant interference is $^{16}O_2{}^+$, though other interferences such as $^{14}N^{18}O^+$ and $^{15}N^{16}O^1H^+$ should be considered. There are two possible approaches to chemical resolution of interferences: one can either react the interfering ion to remove it from the m/z of interest or react the ion of interest in order to detect a product ion at a new, noninterfered m/z. Let us consider the thermochemical properties of the relevant ions with the view to employing charge-transfer, hydrogen atom-transfer, or oxidation reactions. Atom affinity and bond strengths in Tables 1 and 2, respectively, were calculated as enthalpy changes of the corresponding association or dissociation reaction using available thermochemical data.[9]

It is clear that resolution by charge-exchange reaction can only be possible for S^+/O_2^+, as the ionization potentials of NO and NOH are lower than those of P and S so that charge transfer that is favorable for the interference is also favorable for the analyte ions. H-atom transfer could only be useful for converting analytes to PH^+ and SH^+ by reaction with C_2H_4 (the only indicated gas with suitable hydrogen bond strength); however, NOH^+ and O_2^+ both have higher affinity to H than does C_2H_3 and thus may form NOH_2^+ and O_2H^+, respectively.

Table 3. Reaction Data for P^+ and S^+ and Relevant Interfering Ions

no.	reaction	reaction enthalpy change ΔH_r, kcal/mol	thermal reaction rate constant k_r, molecule^{-1} cm^3 s^{-1}
1	$P^+ + O_2 \rightarrow PO^+ + O$	−71.4	5.3×10^{-10}
2	$S^+ + O_2 \rightarrow SO^+ + O$	−6.2	1.8×10^{-11}
3	$CO^+ + O_2 \rightarrow CO_2^+ + O$	−13.5	$<2 \times 10^{-14}$ (no reaction)
4	$HCO^+ + O_2 \rightarrow COOH^+ + O$	3.3	$<2 \times 10^{-13}$ (no reaction)
5	$NO^+ + O_2 \rightarrow NO_2^+ + O$	57.4	$<1 \times 10^{-11}$ (no reaction)
6	$NOH^+ + O_2 \rightarrow NO_2H^+ + O$	19.3	no data
7	$O_2^+ + O_2 \rightarrow O_3^+ + O$	102.1	no data
8	$Ti^+ + O_2 \rightarrow TiO^+ + O$	−46.1	5.0×10^{-10}

The prominent difference between the analytes and all interferences is seen in their O-atom affinity. O-atom transfer from O_2 to P^+ and S^+ is thermodynamically allowed while for NO^+, NOH^+, and O_2^+ it is endothermic and thus forbidden under thermal conditions. Table 3 gives the reaction enthalpy changes (calculated using thermochemical data[9]) and rate constants reported[10] for the relevant reactions.

Reactions for P^+ and S^+ are both exothermic, with P^+ reacting faster than S^+. Oxidation reactions for HCO^+, NO^+, NOH^+, and O_2^+ with O_2 are endothermic and cannot proceed under thermal conditions, O_2^+ is reported to react only by charge transfer. The exothermic reaction of CO^+ leading to CO_2^+ is reported as not proceeding. We also give here for reference the data for Ti^+, which can potentially interfere with PO^+ and SO^+. Ti^+ is removed to its oxide by the same reaction gas at approximately the same rate as PO^+ formation.

It is conceivable that other atom- or radical-transfer reactions may be suitable for converting P^+ and S^+ to new analyte ions. We have attempted oxidation with N_2O and CO_2, fluorination with CH_3F, chlorination with CH_3Cl, and methylation with CH_4, C_2H_4, and C_2H_6. However, the resultant background equivalent concentrations and detection limits with any of these gases were many times worse than with oxygen and are not reported here.

EXPERIMENTAL SECTION

The instrument used in these studies (PerkinElmerSCIEX Elan DRC) has been described elsewhere.[11] Microflow PFA-ST nebulizers (200 and 20 μL/min) and a Teflon spray chamber (Elemental Scientific Inc.) were used. Research purity (99.998%) oxygen (Matheson Gas Products, Whitby, ON, Canada) was used as reaction gas. Samples of S, P, and Ti were prepared from 1000 μg/mL PE Pure single-element standard solutions (PerkinElmer, Shelton, CT) by sequential dilution with high-purity deionized water (DIW) produced using a Elix/Gradient (Millipore, Bedford, MA) water purification system. Other reagents used were AnalaR

(9) Lias, S. G.; Bartmess, J. E.; Liebman, J. F.; Holmes, J. L.; Levin, R. D.; Mallard, W. G. *J. Phys. Chem. Ref. Data* **1988**, *17* (Suppl. 1).

(10) Anicich, V. G. Ion reactions databases. *Astrophys. J., Supple. Ser.* **1993**, *84*, 215. Also, http://astrochem.jpl.nasa.gov/asch/.

(11) Baranov, V. I.; Tanner, S. D. *J. Anal. At. Spectrom.* **1999**, *14*, 1133−1142.

Table 4. Experimental Conditions for Optimum Signal-to-Background Ratio for PO^+ and SO^+ Detection in DIW for ELAN DRC

parameter	value	parameter	value
plasma gas, Ar, L/min	15	cell rod offset (CRO), V	−1
auxiliary gas, Ar, L/min	1	analyzer rod offset (QRO), V	−6.5
nebulizer gas, Ar, L/min	1.02 (max signal) 1.05 (for DIW)	cell gas A, units	0
plasma power, W	1100	cell gas B (O_2), units	0.75
lens voltage, V	5.1 (fixed)	DRC Mathieu parameter a (RPa)	0.02
cell path voltage (CPV), V	−17	DRC Mathieu parameter q (RPq)	0.40
nebulizer	microconcentric PFA 200 (ESI)	spray chamber	PFA, Scott double pass (ESI)

grade acetonitrile, Aristar grade formic acid and AnalaR grade ammonium bicarbonate (all three from BDH Inc., Toronto, ON, Canada). Bovine milk β-casein, α-casein, and dephosphorylated α-casein were purchased from Sigma-Aldrich Canada Ltd. (Oakwille, ON, Canada).

The measurements were conducted in a class 1000 clean room, with the sample introduction system protected by a class 100 portable laminar flow bench.

One of the two instruments used in the study was upgraded to an Elan DRC^{PLUS} in order to assess the effects of an axial field within the reaction cell. An oxygen getter purifier (NuPure Corp., Ottawa, ON, Canada) was used on the upgraded instrument; however, no effect of the getter on the results was noticed. It might be noted that, although extreme precautions were taken to avoid contamination, the method of P and S determination described here also was used with similar results on a third instrument, with UHP grade (99.98% minimum) oxygen (Matheson Gas Products) and not in the clean room, having only a class 1000 laminar flow bench to protect the sample introduction system.

Optimization. The instruments were optimized to provide standard operating conditions (see Table 4) in standard mode (DRC vented), and then oxygen was bled into the closed reaction cell at a flow of 1 arbitrary unit for 30−60 min, after which the reaction gas flow, nebulizer gas flow, RPq, and RPa (the q and a rf stability parameters of the DRC, respectively) were optimized. It is obvious that a relatively low value of RPq (i.e., wide band-pass[12]) is to be used in order to simultaneously transmit m/z = 31 and 50 (recall that the mass band-pass widens as RPq is reduced). It was found that a nonzero RPa (0.02) was beneficial for the optimal background equivalent concentration. We think that the background at m/z = 47−50 is not likely to originate from heavier ions for which the high-mass cutoff (principally defined by nonzero RPa) may provide beneficial suppression. Rather, we attribute the effect of RPa to the change in the "sharpness" of the stability boundaries, such that low-mass precursors are rejected more efficiently when RPa is slightly nonzero. Operating at a relatively wide band-pass allows some products of sequential side reactions to survive and produce a background at m/z = 45−50. It is likely that these background ions are the products of reactions initiated by charge exchange between O_2 and the dominant plasma ions, because increasing the nebulizer flow rate beyond optimal sensitivity improves the background equivalent concentrations and detection limits. Operating with slightly higher than optimum nebulizer gas flow favorably reduces the ratio of those dominant ions to the P^+ and S^+.

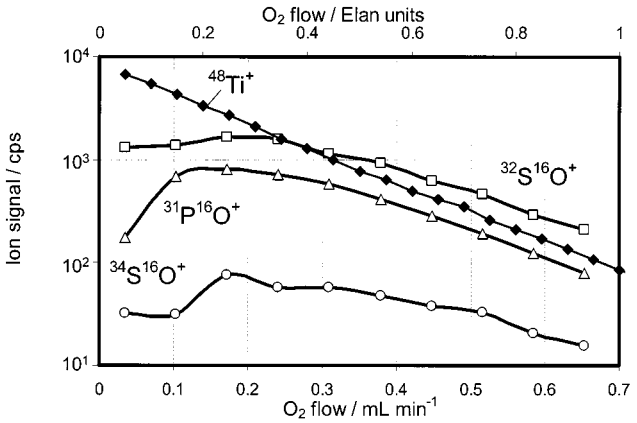

Figure 1. Net signals (blank subtracted; counts/s, cps) for $^{31}PO^+$ and $^{32}SO^+$ as a function of oxygen flow rate for a sample of 10 ng/mL in DIW. Reaction profile for Ti^+ measured for a separate sample is also shown.

Figure 1 shows oxygen gas optimization for product ions PO^+ and SO^+ for a sample containing 10 ng/mL P and S. Also given in Figure 1 is the reaction profile for Ti^+ oxidation. Thus, the method can be to a certain degree tolerant of the presence of some Ti^+ in the sample. Normally, one would not expect much Ti in biological samples, and care should be taken to ensure that the buffers and reagents used in sample preparation do not contain it. The instrument was optimized for the best background equivalent concentration (Figure 2), leading to the conditions given in Table 4. Under these conditions, the limits of detection (3σ, 5-s integration) for P and S measured as $^{31}PO^+$ and $^{32}SO^+$ are 0.20 and 0.52 ng/mL, with background equivalent concentrations of 0.53 and 4.8 ng/mL, respectively.

Figure 3 shows mass spectra for a sample containing P and S at 10 ng/mL and for a blank (deionized water). We are not able to identify the species that define the background at m/z = 45−50. The 48/50 ratio is consistent with some S impurity in DIW. A combination of $CO_2H_n^+$ and NO_2H^+ may contribute to the background at m/z = 45 and 46. Nevertheless, as oxidation reactions of the interferences are endothermic, the background equivalent concentration and detection limits are improved significantly when compared to standard mode.

When organic matrix (5% CH_3CN + 5% CH_2O_2 + 1 mM NH_4HCO_3) is introduced, the signal maximum for P^+ and S^+ shifts

(12) Tanner, S. D.; Baranov, V. I. J. *Am. Soc. Mass. Spectrom.* **1999**, *10*, 1083−1094.

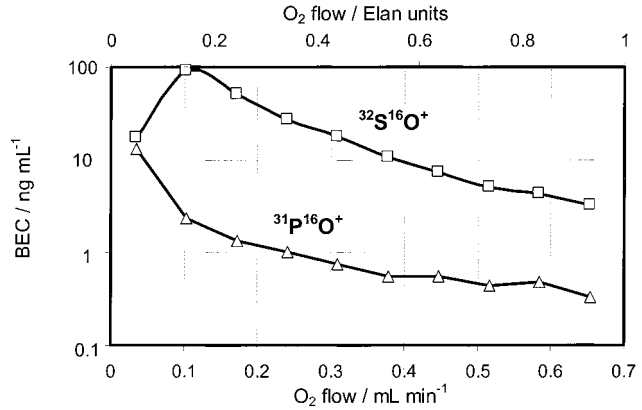

Figure 2. Equivalent concentration of the blank (DIW) for $^{31}PO^+$ and $^{32}SO^+$ as a function of oxygen flow.

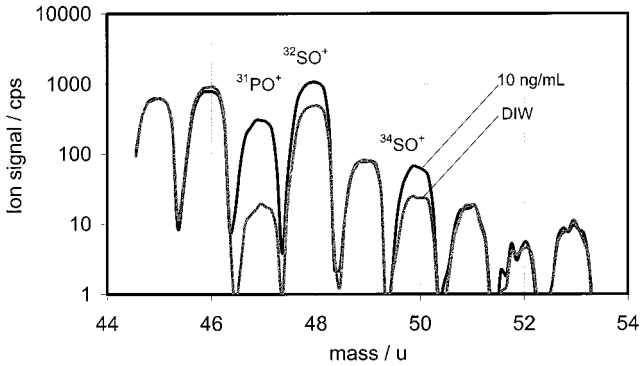

Figure 3. Mass spectra for 10 ng/mL P and 10 ng/mL S sample and blank (DIW) measured with instrument parameters as per Table 4.

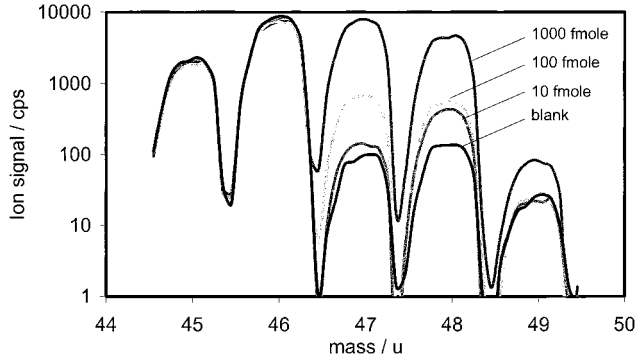

Figure 4. Mass spectra of a protein β-casein for 0, 10, 100, and 1000 fmol/μL in a digest buffer (5% CH_3CN + 5% CH_2O_2 + 1 mM NH_4HCO_3).

to lower nebulizer flow due to changes in the plasma temperature. In this instrument, it is thought that most of the background corresponds to polyatomic ions of the incompletely atomized matrix. Decreasing the nebulizer flow rate improves matrix decomposition. For organic matrixes, optimum BEC is achieved at a lower nebulizer flow than that which provides maximum analyte intensity.

Figure 4 shows spectra of a protein β-casein for 0, 10, 100, and 1000 fmol/μL in the digest buffer (5% CH_3CN + 5% CH_2O_2 + 1 mM NH_4HCO_3). A calibration curve derived from these data for P and for phosphorus standard additions (5, 50, and 100 ng/mL or 161.3, 1613, and 3226 fmol/μL ^{31}P, respectively) to the 1000 fmol/μL sample are given in Figure 5. The PO^+ response is linear

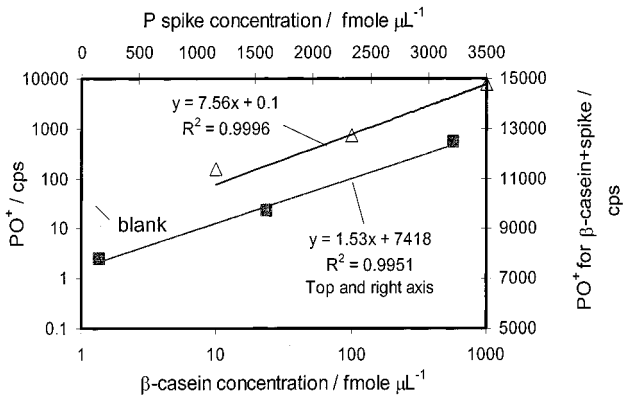

Figure 5. $^{31}PO^+$ calibration curve for β-casein (triangles, left and bottom axis) and response for P standard additions to the sample of 1000 fmol/μL β-casein (squares, right and top axis). Ratio of slopes characterizes the degree of phosphorylation.

in this range of concentrations. From the slopes of the lines, one can estimate the degree of phosphorylation of β-casein, $N_P = 7.56/1.53 = 4.94$ mol/mol.

It is known that bovine milk β-casein molecule is phosphorylated at five serine residues (amino acids 30, 32−34, and 50 in the sequence) except for variant C (which is phosphorylated only at four serines 30, and 32−34).[13] Thus, agreement of ICP-DRC-MS quantitation with existing sequence knowledge is remarkable.

Effect of Axial Field. Although the detection limits of the method are significantly better than for nonreaction cell quadrupole ICPMS, the sensitivity (about 50 and 100 (counts/s)/ppb for P and S, respectively) is inferior to what is usually expected from ICPMS. Partially this is due to the high ionization potential of P and S, which results in a relatively low degree of ionization in the ICP, 33% and 14%, respectively.[14] Another source of significant loss of sensitivity is collisional scattering of the parent and product ions with the relatively heavy reaction gas. Introduction of a dc axial field to "herd" ions through the reaction cell reduces scattering losses. The particulars of the instrument equipped with the axial field cell (DRC^{PLUS}) were described recently[15] and are the subject of a separate paper currently in preparation. The cell has additional auxiliary electrodes[16,17] inserted between the quadrupole rods, which provide axial field of ~0.2 V/cm when biased to a dc potential of +200 V. Figure 6 shows the effect of axial fields of varying strength on the backgrounds and signals at m/z = 47, 48, and 50 for the blank (DIW) and for a sample containing 10 ng/mL P and S. At an axial field potential (AFP) of 275 V, sensitivity is enhanced by a factor of 4−6 compared to the same cell operated with no axial field (AFP = 0 V) or compared to the DRC (see Figure 1). The background equivalent concentration (BEC) for $^{32}SO^+$ at m/z = 48 is reduced by the field, while for

(13) Swiss- Prot Protein Knowledgebase, hosted by SIB Switzerland, http://www.expasy.ch/sprot/.
(14) Houk, R. S. *Anal. Chem.* **1986**, *58*, 97A−105A.
(15) Bandura, D. R.; Baranov, V. I.; Tanner, S. D. Dynamic Reaction Cell with Axial Field. Presented at the 47th International Conference on Analytical Sciences and Spectroscopy, Toronto, August 19−21, 2001.
(16) Thomson, B. A.; Jolliffe, C. L. Spectrometer With Axial Field. U.S. Patent 5,847,386, 1998.
(17) Loboda, A.; Krutchinsky, A.; Loboda, O.; McNabb, J.; Spicer, V.; Ens, W.; Standing, K. Novel Linac II Electrode Geometry to Create an Axial Field in a Multipole Ion Guide. Presented at the 48th ASMS Conference on Mass Spectrometry and Allied Topics, Long Beach, CA, June 11−15, 2000.

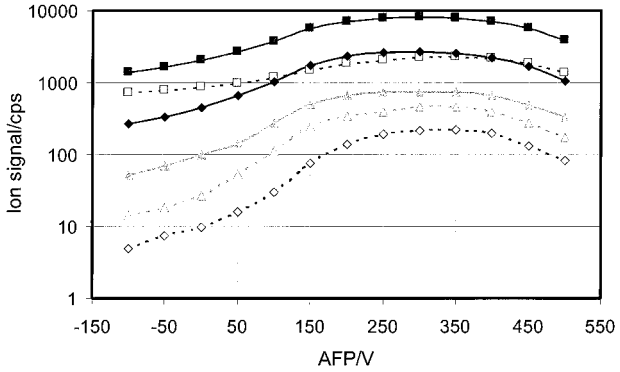

Figure 6. Signals for PO^+ and SO^+ vs axial field potential at O_2 = 0.5 arbitrary unit, RPq = 0.4, RPa = 0.02, and nebulizer flow of 200 μL/min. Solid symbols and lines, 10 ng/mL P and S sample; open symbols and dotted lines, blank (DIW). Diamonds, m/z = 47; squares, m/z = 48; triangles, m/z = 50.

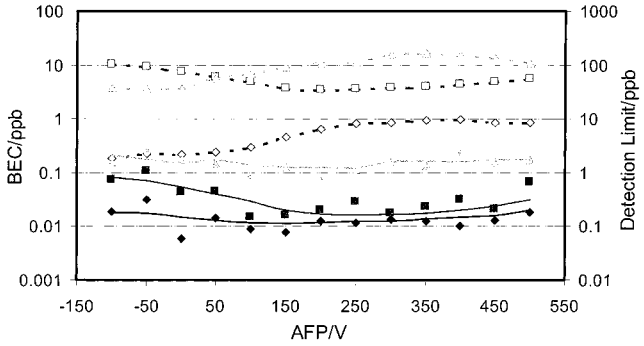

Figure 7. Background equivalent concentration (BEC, open symbols and dotted lines), estimated detection limit (EDL, 3σ, 2 s, solid lines), and measured detection limit (3σ, 7 replicates × 2 s, solid symbols) for P and S measured as PO^+ and SO^+ vs axial field potential (AFP). O_2 = 0.5 arbitrary unit, RPq = 0.4, RPa = 0.02, and nebulizer at 200 μL/min. Diamonds, PO^+; squares, $^{32}SO^+$; triangles, $^{34}SO^+$.

$^{34}SO^+$ at m/z = 50 and for PO^+ at m/z = 47 (BEC), it is increased (Figure 7). However, as the increase in BEC scales slower than the square of the increase of the sensitivity, the detection limits at optimum AFP are slightly improved for $^{34}SO^+$ and PO^+ and more than 2 times better for $^{32}SO^+$. We attribute this improvement to possible suppression of the condensation reaction

$$O^+ + O_2 = O_3^+ \qquad (9)$$

which, although thermodynamically allowed ($\Delta H_r = -52.6$ kcal/mol), requires a third collision partner to absorb the energy released in the reaction (otherwise, the excited O_3^{*+} intermediate will dissociate). Although precursor O^+ is unstable when m/z = 48 is measured at RPq = 0.4, its intensity is extremely high (similar to that of Ar^+) and thus some of the ions experience reactive collisions before being rejected due to instability in the rf field. When an axial field is employed, the average ion velocity is increased, and thus, the lifetime of the intermediate and the probability of third body stabilization is reduced. We attempted to employ in situ energy discrimination with a retarding axial field (negative AFP), hoping to see greater kinetic energy discrimination against polyatomic ions such as O_3^+, NO_2^+, and $CO_2H_n^+$.

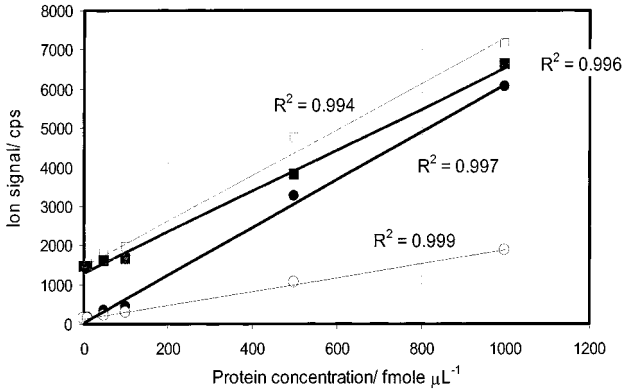

Figure 8. Calibration for regular (solid symbols) and dephosphorylated (open symbols) α-casein. O_2 = 0.5, RPq = 0.4, RPa = 0.02, and micronebulizer at 16 μL/min. Circles, PO^+; squares, $^{32}SO^+$.

However, the production of O_3^+ appears to increase when the ions are slowed by the deceleration field, which supports the mechanism suggested.

Figure 7 shows estimated detection limits (EDL) and measured instrument detection limits (IDL) that are calculated as

$$\mathrm{EDL} = 3\sqrt{N_s}/((N_s - N_b)\sqrt{t})C_s \qquad (10)$$

$$\mathrm{IDL} = 3\mathrm{SD}_b/(N_s - N_b)C_s \qquad (11)$$

where N_s and N_b are measured signals (counts per second) at the m/z of interest for sample and blank, respectively, and SD_b is the standard deviation of the blank, for integration time t = 2 s. The measured detection limits follow closely the EDL and reach ≤0.1 ng/mL for P and ≤0.2 ng/mL for S, at <1 and <4 ng/mL BEC, respectively. For longer integration (5 s), detection limits of 0.06 ng/mL for P and 0.19 ng/mL for S were measured. P and S are measured simultaneously; S can be used as an "internal" standard to assess the total amount of the proteins or other biological material in the sample, valid for homologous proteins and in instances where the S content is proportional to protein concentration.

Degree of Phosphorylation of α-Casein. An example where this assumption is expected to hold is the comparison of homologous proteins having different states of phosphorylation. Figure 8 shows calibration curves for P and S measured for regular and dephosphorylated α-caseins at 0, 10, 50, 100, 500, and 1000 fmol/μL in 5% acetonitrile (v/v). A low-flow micronebulizer (16 μL/min) was used in order to reduce the amount of sample used. The responses are linear in this range of concentrations, and the relative difference in the phosphorus concentration can be assessed through the P/S ratio. The instrument response in 5% acetonitrile was measured at 22.4 (counts/s)/(ng/mL) for P and 30.5 (counts/s)/(ng/mL) for S (note that the sensitivity is much lower at a sample uptake of 16 μL/min than at the 200 μL/min used earlier). Accounting for the instrument response factor, the ratio P/S for regular α-casein is 1.58, and for dephosphorylated α-casein it is 0.41. Regular bovine milk α-casein is known to have 8−10 phosphorylation sites and 5−7 methionines and cysteines (depending on genetic variant).[13] Thus, the measured ratio P/S and number of phosphorus atoms per molecule of α-casein are in good agreement with the protein structure data.

The difference in P/S ratio indicates ~26% residual phosphate in the dephosphorylated α-casein. These results, which are independent of the concentration of the protein in the sample, agree with direct determination using the calibration curves (that do require knowledge of the concentration).This directly determined P content is 8.8 mol/mol for regular α-casein and 2.5 mol/mol for dephosphorylated α-casein**,** which means 28% residual phosphate for dephosphorylated α-casein.

CONCLUSIONS

It is shown that use of the PO^+ and SO^+ products of oxidation of P^+ and S^+ with O_2 in the DRC as analyte ions reduces the effect of isobaric interferences and allows subnanogram per milliliter detection of P and S in aqueous samples with a low-resolution (quadrupole) analyzer. Use of a dc axial field in the DRC improves sensitivity and detection limits due to more efficient transmission of the product ions through the cell when pressurized with a relatively heavy reaction gas (O_2). Under optimum conditions, detection limits for P and S in aqueous solution of <0.1 and <0.2 ng/mL, respectively, are achieved. It was shown that the method can be used for determining the degree of phosphorylation of β-casein and of regular and dephosphorylated α-casein in the range of concentrations of 10− 1000 fmol/μL, with organic solvents and buffers present in the sample at a level of 5−15%. The measured concentration of P and P/S ratio for regular α-casein were in good agreement with the protein structure. Dephosphorylated α-casein was measured to have 26−28% residual phosphate.

ACKNOWLEDGMENT

The authors thank Dr. Olga Ornatsky of MDS Proteomics and Dr. Zoe Quinn of MDS SCIEX for sharing their knowledge and expertise in biochemistry.

Received for review September 26, 2001. Accepted December 31, 2001.

AC011031V